Macroscopic and microscopic wettability of graphene

Belyaeva, L.A.; Tang, C.; Juurlink, l.; Schneider, G.F.

LANGMUIR

pubs.acs.org/Langmuir Article

Macroscopic and Microscopic Wettability of Graphene

Liubov A. Belyaeva, Chen Tang, Ludo Juurlink, and Grégory F. Schneider*

Cite This: *Langmuir* 2021, 37, 4049–4055

Read Online

ACCESS | Metrics & More | Article Recommendations

ABSTRACT: Interactions between water and graphene can be probed on a macroscopic level through wettability by measuring the water contact angle and on a microscopic level through water desorption kinetic studies using surface science methods. The contact angle studies of graphene pinpointed the critical role of sample preparation and measurement conditions in assessing the wettability of graphene. So far, studies of water desorption from graphene under the conditions of ultrahigh vacuum provided superior control over the environment but disregarded the importance of sample preparation. Here, we systematically examined the effect of the morphology of the growth substrate and of the transfer process on the macroscopic and microscopic wettability of graphene. Remarkably, the macroscopic wetting transparency of graphene does not always translate into microscopic wetting transparency, particularly in the case of an atomically defined Cu(111) substrate. Additionally, subtle differences in the type of substrates significantly alter the interactions between graphene and the first monolayer of adsorbed water but have a negligible effect on the apparent macroscopic wettability. This work looks into the correlations between the wetting properties of graphene, both on the macroscopic and microscopic scales, and highlights the importance of sample preparation in understanding the surface chemistry of graphene.

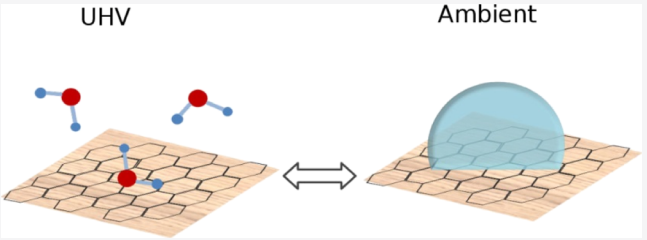

INTRODUCTION

The subject of wettability of graphene has been widely studied but, nonetheless, remains under ongoing debate.[1−3] Understanding and taking control of the wetting behavior of graphene would benefit the wide range of graphene applications—sensors, nanoelectronics, fuel cells, and so forth.[4−9] However, there exists a remarkable discrepancy in the reported contact angles of graphene, varying from being very hydrophilic when supported by water[10] to mildly hydrophilic on glass[11] and to hydrophobic on silicon carbide and copper.[12,13] In general, three factors determine the wetting properties of graphene:[3] the intrinsic wettability of graphene, the effect of the underlying substrate, that is, the wetting transparency of graphene,[11,14,15] and the sample preparation-related environmental factors, such as morphological features and defects caused by the growth and transfer processes,[16] contamination, and adsorption of airborne hydrocarbons.[17] Furthermore, while the intrinsic contact angle of clean freestanding graphene has already been determined to be 42 ± 3° both theoretically[18,19] and experimentally,[20] the effects of the substrate and environment are difficult to disentangle. As a result of the diversity of growth and handling conditions, graphene has been independently shown to be fully transparent,[11] partially transparent,[15] and fully opaque to wetting.[12,21] Particularly, irregularities in the graphene structure caused by the transfer appear paramount for the disruption of the wetting transparency.[10]

In addition to contact angle measurements, another route to approach the wettability of graphene is to study water desorption using surface science methods, such as temperature-programed desorption (TPD)[22]—also referred to as thermal desorption spectroscopy.[23,24] Contrary to the macroscopic contact angle measurements in ambient atmosphere, TPD probes interactions between a surface and isolated molecules, sheets, or clusters of water molecules under ultrahigh vacuum (UHV) conditions and characterizes the so-called "wettability on a molecular level". The wettability on a molecular level, however, does not necessarily correlate with the apparent macroscopic wettability (e.g., in the case of silver and gold) but complements the macroscopic observations. Macroscopic wettability observed in ambient atmosphere involves significantly larger number of collisions and interactions between molecules (both of water and environment) than microscopic wettability observed in UHV.[25] As for studies involving contact angle measurements, several TPD studies of graphene showed contrasting results on the wetting transparency (on the molecular level) of graphene, particularly, graphene on Ru(0001), Cu, and Si/SiO_2 was shown to be

Received: September 25, 2020
Revised: February 17, 2021
Published: March 2, 2021

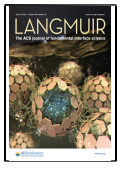

https://doi.org/10.1021/acs.langmuir.0c02817
Langmuir 2021, 37, 4049−4055

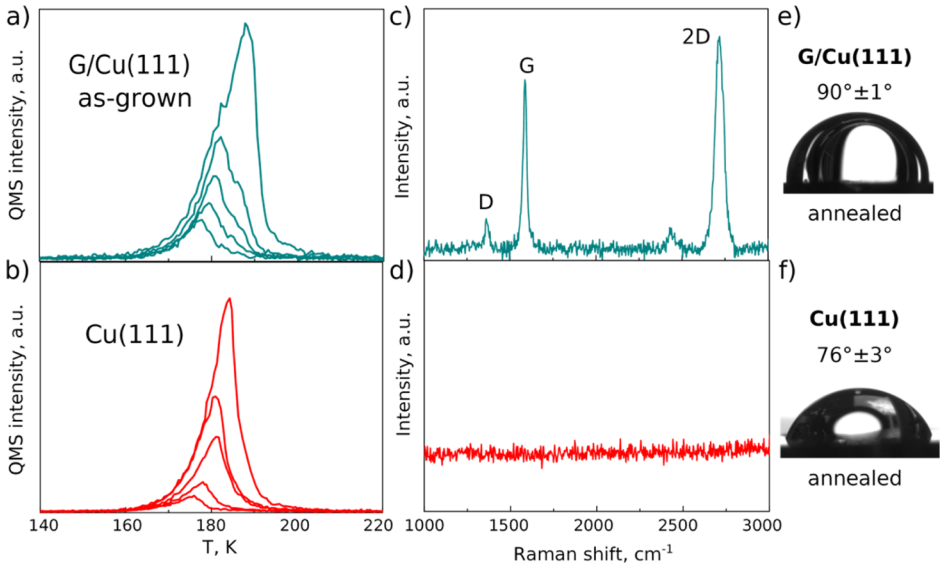

Figure 1. Microscopic and macroscopic wettability of graphene grown on Cu(111). (a) TPD curves of graphene grown on Cu(111) at submonolayer coverages. Each curve corresponds to the different amount of water injected and adsorbed onto the surface, yielding 0.3−1.2 surface coverages (from the bottom to the top curve), respectively. (b) TPD curves of bare Cu(111) at submonolayer coverages. Each curve corresponds to the different amount of water injected and adsorbed onto the surface, yielding 0.3−1.2 surface coverages (from the bottom to the top curve), respectively. (c) Typical Raman spectrum of graphene grown on Cu(111). (d) Typical Raman spectrum of bare Cu(111) after graphene removal by argon sputtering. (e) Water contact angle of graphene grown on Cu(111) measured immediately after annealing. (f) Water contact angle of unoxidized Cu(111) measured immediately after annealing.

opaque in water desorption measurements[23,24,26] but nearly transparent in the benzene desorption measurements (with the exception of graphene on Ru(0001) which was opaque in both cases).[27] A theoretical study also demonstrated the prominent substrate effect on the water desorption on graphene by investigating the electronic properties of graphene upon water adsorption.[28] Given the extreme accuracy and cleanness of the measurements under UHV, the reported discrepancies in the microscopic wettability of graphene distinctly point at the crucial role of sample preparation preceding the desorption experiments.[3]

In this article, we studied the influence of the crystallinity of the substrate and of the transfer process on the wettability and wetting transparency of graphene, both at the macroscopic (ambient) and microscopic (vacuum) levels. The same samples were used for contact angle measurements and TPD, allowing, therefore, for a direct comparison between macroscopic wettability and water desorption in vacuum. Remarkably, although graphene is wetting transparent macroscopically regardless of the preceding treatment, desorption measurements showed that the morphology of the substrate and transfer-induced irregularities significantly alter the interactions between graphene and the first monolayer of water molecules.

RESULTS

Three different samples were studied comparatively by contact angle measurements and TPD: (i) graphene as-grown on Cu(111), (ii) graphene as-grown on polycrystalline copper, and (iii) graphene transferred to a polycrystalline copper substrate. The bare polycrystalline copper and Cu(111) were also tested after the graphene layer was removed by argon sputtering in UHV. The as-grown samples were prepared using the chemical vapor deposition (CVD) method, and the transferred sample was first grown on a different copper foil according to the same CVD protocol and then transferred to polycrystalline copper using the poly(methyl methacrylate) (PMMA)-assisted transfer method (see Methods for more details). Then, the samples were studied using TPD at various water coverages on graphene. After each measurement, the graphene layer was removed directly from the UHV chamber by sputtering, and water desorption from the bare copper substrates was also studied using identical procedures (see Methods).

As copper quickly oxidizes once exposed to air, contact angles were measured for bare copper crystals after annealing in hydrogen atmosphere (i.e., within 1−2 min) and 30 min after the annealing. No oxide layer was formed in the samples of as-grown graphene on copper because during CVD graphene grows on copper directly in a vacuum without exposure to air. However, to remove the adsorbed airborne hydrocarbons,[17] all graphene samples were also annealed right before measuring the contact angle.

Graphene Grown on Cu(111). In a typical TPD experiment, a specific amount of water (predetermined by the change in pressure) is injected into the UHV chamber at a low temperature (~100 K in our case), which adsorbs onto the surface of the sample. Furthermore, the sample is heated, and the amount of desorbing water molecules is recorded as a function of temperature, yielding a desorption curve (Figure 1a,b). Several experiments at different amounts of injected water are typically carried out, yielding a set of desorption curves recorded for each sample. Both monolayer and multilayer adsorption of water on the surface (or surface coverage) can be studied; however, the curves recorded for submonolayer coverages are the most informative for the characterization of water−surface interactions. The shape of the curves, the onset temperature, and their change with increasing coverage are linked to the kinetic and thermodynamic characteristics of water−surface interactions, such as binding energy, kinetic order of desorption (provides

https://doi.org/10.1021/acs.langmuir.0c02817
Langmuir 2021, 37, 4049−4055

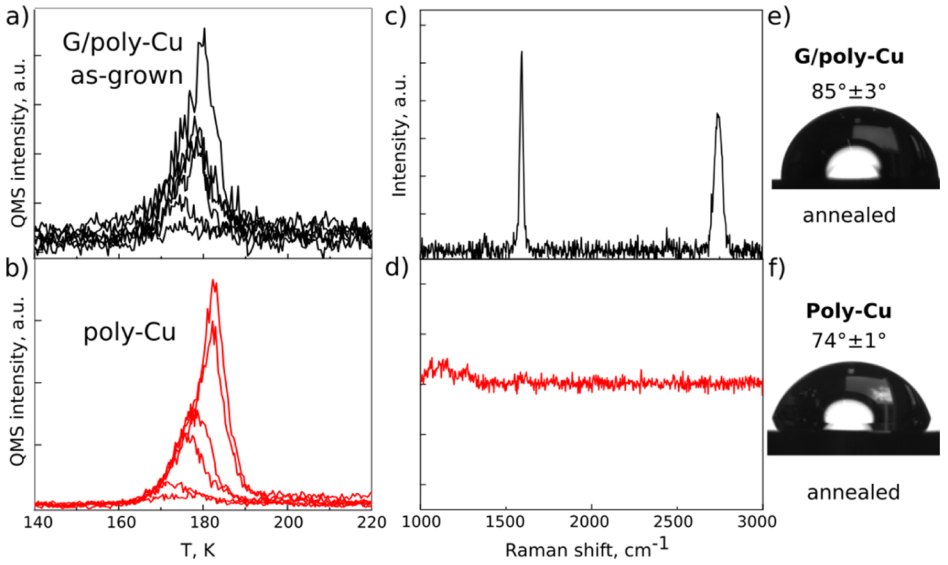

Figure 2. Microscopic and macroscopic wettability of graphene grown on polycrystalline Cu. (a) TPD curves of graphene grown on polycrystalline Cu at submonolayer coverages. Each curve corresponds to the different amount of water injected and adsorbed onto the surface, yielding 0.3−1.2 surface coverages (from the bottom to the top curve), respectively. (b) TPD curves of bare polycrystalline Cu at submonolayer coverages. Each curve corresponds to the different amount of water injected and adsorbed onto the surface, yielding 0.3−1.2 surface coverages (from the bottom to the top curve), respectively. (c) Typical Raman spectrum of graphene grown on polycrystalline Cu. (d) Typical Raman spectrum of bare polycrystalline Cu after graphene removal by argon sputtering. (e) Water contact angle of graphene grown on polycrystalline Cu measured immediately after annealing. (f) Water contact angle of polycrystalline Cu measured right after annealing. Abbreviation: QMA, quadrupole mass spectrometer.

information about adsorption mechanism and ordering of water molecules), and desorption energy.[3,29]

Figure 1a,b shows that graphene grown on Cu(111) is not fully transparent to water desorption. Specifically, although graphene on Cu(111) and on bare Cu(111) show the same onset desorption temperature T_{onset} close to 160 K, their kinetic characteristics differ significantly. A shared leading edge and a shift to higher temperatures with the increase in coverage, as in Figure 1a, indicate a zero-order desorption in the case of graphene on Cu(111), and the mixed features of the zero- and first-order kinetics in Figure 1b indicate a fractional order desorption (between 0 and 1) for bare Cu(111). The zero-order kinetics in the case of graphene on Cu(111) is ascribed to the two-dimensional equilibrium between individual water molecules and islands of condensed water[22,30] and, thus, indicates that water tends to form multilayer clusters rather than a continuous monolayer on graphene. Contrastingly, the fractional kinetic order for bare Cu(111) shows that the copper surface is more favorable (compared to graphene on Cu(111)) to the adsorption of water molecules.

The adsorbed thin water film also seems structured differently on graphene on Cu(111) and bare Cu(111). While the shape of the desorption curves for bare Cu(111) is smooth, the desorption curves of graphene on Cu(111) display a clear "bump" on their descending edge (Figure 1a). It broadens the desorption significantly. Such a change in desorption rate is reminiscent of the crystallization of metastable amorphous water ice to crystalline ice.[22,31−33]

The Raman spectra in Figure 1c confirmed that graphene is monolayered with a sharp 2D mode and a negligible defect-related D mode. The absence of graphene bands in Figure 1d indicates that graphene was completely removed from copper after argon sputtering.

As seen from the contact angle measurements in Figure 1e,f, the addition of a graphene layer did not significantly change the mildly hydrophilic behavior of Cu(111): angles of 90 ± 1° for graphene grown on Cu(111) (Figure 1e) and 76 ± 3° for bare nonoxidized Cu(111) (Figure 1f) were measured. Although the difference is statistically significant, it is only slightly bigger than the standard deviation. However, the slightly more hydrophobic behavior of graphene on Cu(111) does coincide with the lower affinity of graphene to water on a molecular level observed in TPD.

Although there seems to be a discrepancy in the contact angles of copper in the literature (ranging from 0 to 90°), we must note that the contact angle measured in ambient conditions has been consistently reported to be around 70−80°, that is, in agreement with our results.[10,11,34−36] Interestingly, the contact angle measured in the "microscopic regime"—in UHV and with thoroughly degassed and deoxygenated water—and on ultrapure copper was 0°.[37] The exact reasons behind the difference between macroscopic wettability in ambient atmosphere and UHV are not fully identified and can include: the difference in pressure, formation of a copper oxide layer in an ambient atmosphere, different physisorption characteristics of nonwater molecules in vacuum and an ambient atmosphere, and possible chemical reactions between water molecules and copper in vacuum.[37]

Graphene As-Grown on Polycrystalline Cu. Unlike graphene on Cu(111), graphene grown on polycrystalline copper is transparent to water desorption (Figure 2). The water desorption curves from graphene as-grown on polycrystalline copper and bare copper (Figure 2a,b) display the same onset temperature, T_{onset}, at 160 K (also equal to that of graphene on Cu(111) and bare Cu(111)). The desorption curves show similar shapes with overlapping leading edges. This behavior is representative of zero-order desorption kinetics.[22,30] The strictly overlapping onsets and absence of

https://doi.org/10.1021/acs.langmuir.0c02817
Langmuir 2021, 37, 4049−4055

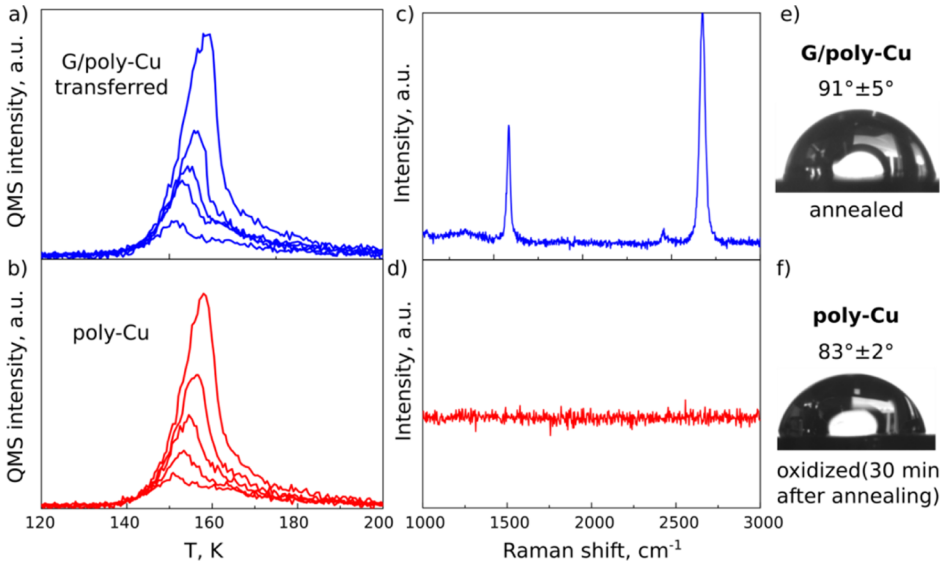

Figure 3. Microscopic and macroscopic wettability of graphene transferred on polycrystalline Cu. (a) TPD curves of graphene transferred on polycrystalline Cu at submonolayer coverages. Each curve corresponds to the different amount of water injected and adsorbed onto the surface, yielding 0.3−1.2 surface coverages (from the bottom to the top curve), respectively. (b) TPD curves of bare polycrystalline Cu after graphene removal at submonolayer coverages. Each curve corresponds to the different amount of water injected and adsorbed onto the surface, yielding 0.3−1.2 surface coverages (from the bottom to the top curve), respectively. (c) Typical Raman spectrum of graphene transferred on polycrystalline Cu. (d) Typical Raman spectrum of bare polycrystalline Cu after graphene removal. (e) Water contact angle of graphene transferred on polycrystalline Cu measured immediately after annealing. (f) Water contact angle of oxidized polycrystalline Cu measured 30 min after annealing.

"bumps" on the leading or descending edges suggest that the water overlayer on polycrystalline Cu is not affected by graphene, in contrast to what we observed on Cu(111).

Contact angle measurements, on the other hand, showed that bare and graphene-coated polycrystalline copper substrates have similar contact angles (74 ± 1 and 85 ± 1°, respectively, Figure 2e,f), suggesting that graphene is nearly transparent macroscopically when grown on polycrystalline copper. Interestingly, the equality of T_{onset} = 160 K for the polycrystalline copper and Cu(111) is consistent with the similar measured contact angles (i.e., 74 ± 1° for annealed polycrystalline copper and 76 ± 3° for annealed Cu(111), Figures 2f and 1f, respectively).

Clearly, the relationships between microscopic and macroscopic wettability of graphene are not straightforward and are difficult to decipher. On one hand, TPD was more sensitive to the morphology of the growth substrate (Cu(111) vs polycrystalline copper) and demonstrated that the morphology of copper affects the interactions between the first layer of adsorbed water molecules and graphene, while the contact angle measurements showed no qualitative difference for graphene on Cu(111) and on polycrystalline copper (a slight increase of the contact angle by ∼10° as compared to the bare substrates indicates that the samples remained mildly hydrophilic). On the other hand, in the case of graphene on polycrystalline copper, the contact angle measurements indicated a difference in the wetting of graphene on copper and of bare copper (Figure 2e,f), while the desorption measurements did not detect any difference in kinetics between the two samples.

Graphene Transferred onto Polycrystalline Copper. Graphene transferred onto the same polycrystalline copper, on one hand, similarly manifests wetting transparency at a molecular level, showing no difference in the desorption behavior between graphene on copper and bare copper (Figure 3a,b). On the other hand, the TPD curves in this case exhibit two features that differ from the as-grown sample: T_{onset} of 140 K and a fractional kinetic order of desorption between 0 and 1 (shift to a higher temperature range with increasing coverage but an ascending leading edge; Figure 3a,b). The difference in T_{onset} may be real but could also be an artifact resulting from the variations in treatments of the samples and their attached thermocouples in the as-grown and transferred experiments. The different kinetics for the two, in principle, identical bare copper substrates in Figures 2 and 3 can be explained by the formation of copper oxide on the top copper layer in the case when graphene was transferred.[38] During the transfer process, the copper crystal is inevitably exposed to air and immersed in water, which are the factors that are known to cause the oxidation of copper.[39] In the case of as-grown graphene, the copper crystal is pre-annealed in hydrogen for 3 h and then immediately followed by the graphene growth in a vacuum, without any exposure to the ambient oxygen. For transferred samples, therefore, the contact angle of the oxidized, that is, exposed to air, copper crystal must be measured for appropriate referencing with TPD results. Similar to the as-grown sample, the contact angle of graphene transferred onto a copper crystal (91 ± 5°, Figure 3e) is close to 83 ± 2° of the oxidized copper crystal after exposure to air (Figure 3f). Interestingly, these values are higher than 74 ± 1° measured for freshly annealed copper (Figure 2f), indicating a more hydrophobic behavior for graphene transferred onto (oxidized) copper and bare (oxidized) copper compared to the as-grown graphene sample and bare nonoxidized copper.

■ CONCLUSIONS

In summary, the effects of substrate crystallinity and the transfer process on the interactions between graphene and water were investigated from both microscopic and macroscopic perspectives. Contact angle measurements showed that the macroscopic wettability of graphene is independent of the

https://doi.org/10.1021/acs.langmuir.0c02817
Langmuir 2021, 37, 4049−4055

substrate crystallinity and transfer, and the addition of a graphene layer on top of copper only slightly increases the contact angle by ∼10°, indicating that graphene manifests nearly wetting transparency in all three samples. Although this increase is statistically significant and, in principle, indicates different wetting properties of graphene/copper compared to those of the bare copper surface (presumably, due to partial screening of polar interactions by graphene[10]), it does not indicate a qualitatively different behavior—that is, contact angles of both 80 and 90° correspond to mildly hydrophilic surfaces. Contrastingly, water desorption measurements demonstrated that the morphology of the substrate and transfer-related imperfections appreciably affect the adsorption of the water monolayer on the graphene surface. In the case of smooth and atomically defined Cu(111), the deposition of a graphene layer resulted in the change of water desorption kinetics, likely resulting from different interfacial and structural properties of the thin water layer in comparison to the case of bare Cu(111). For rougher polycrystalline copper, on the other hand, the deposition of the graphene layer (both by direct growth and transfer) did not alter the kinetic characteristics of copper, manifesting, therefore, wetting transparency on a molecular level. Interestingly, the annealed and oxidized polycrystalline copper crystals have different desorption characteristics (desorption order and perhaps T_{onset}; see Figures 2b and 3b), which are completely retained after the deposition of a graphene layer on top. The difference in the wettability of as-grown and transferred graphene, observed in this work and elsewhere, therefore, seems to stem from the fact that copper is inevitably oxidized in the case of transferred graphene.

As a conclusion, the TPD and contact angle data describe different phenomena and are not perfectly correlated but rather provide complementary insights. Because of the extreme smoothness and homogeneity of the surface of monocrystalline Cu(111), its microscopic wetting properties are readily affected by the addition of a graphene layer, while in the case of polycrystalline copper, the surface properties are dominated by its significant roughness, and the addition of graphene—a monoatomic and fully conforming layer—has a negligible effect.

Interestingly, macroscopic and microscopic wetting transparencies of graphene seem to require different conditions for their breakdown. The macroscopic wetting transparency of graphene has been shown in the literature to be strongly affected (and even completely disrupted) by the transfer process and by the interplay between polar and dispersive interactions[10,40] but not by the crystallinity (orientation of the domains, mono- vs polycrystalline structures, etc.) of the substrate. However, our results suggest that the substrate crystallinity is critical for the occurrence of microscopic wetting transparency of graphene, at least in the case of copper. Copper is known to be a borderline metal between the molecular and dissociative mechanisms of water adsorption.[41] Different crystal modifications of copper have different dominating adsorption mechanisms, suggesting a variety of possible pathways for water−copper bonding and for ordering of water molecules in the first and consequent layers (and therefore for the desorption kinetics).[42−44] While Cu(111) predominantly shows molecular adsorption of water,[42,45] polycrystalline copper shows more dissociative adsorption[42] and oxidized copper (especially polycrystalline) even more dominating dissociative adsorption of water.[43,44] From our results it, therefore, seems that a layer of graphene alters the binding between water molecules and copper in the case of molecular adsorption; however, in the case of dissociative adsorption (and therefore, stronger water−metal interactions) on polycrystalline and oxidized copper, the water−metal binding remains mainly unaffected.

TPD proves very sensitive to the subtle changes in graphene and the underlying substrate (such as crystallinity) and is informative in the scenarios when interactions between graphene and individual molecules of adsorbate are of interest. This information is relevant, for example, for the application of graphene in single-molecule detection[6] and DNA sequencing.[46] Macroscopic wettability measured by contact angle measurements, on the other hand, cannot predict the interactions with individual molecules but, instead, characterizes the interactions between graphene and the macroscopic phases of adsorbate under ambient pressures. This information is relevant for a wide range of graphene applications, for example, coatings, transparent electrodes, field-effect transistors, and others.[4,5,9] Following the recent studies on the effect of sample preparation on the macroscopic wettability of graphene, this work goes further and provides more detailed insights on how different aspects of sample preparation affect the interactions of graphene with individual molecules and with bulk phases.

METHODS

Sample Preparation. All graphene samples were grown using the same CVD protocol.[47] The as-grown samples were grown directly on Cu(111) and on polycrystalline copper substrates that were further studied in TPD. The transferred graphene was first grown on a copper foil and then transferred to a polycrystalline copper substrate using the PMMA-assisted transfer method.[48] All samples were characterized with Raman spectroscopy at an excitation wavelength of 457 nm.

TPD Measurements. TPD experiments were performed in a home-built UHV apparatus with a differentially pumped quadrupole mass spectrometer.[49] The procedure that corrects for the changing background pressure during a TPD experiment has also been described previously.[50] After introducing copper samples with transferred or as-grown graphene into the UHV chamber, the samples were annealed at modest temperatures (∼400 K) to remove the contaminants. Ultrahigh purity water was dosed from a capillary array doser onto the sample. After a series of water TPD spectra for various water coverages on graphene were obtained, graphene was removed by cycles of Ar^+ sputtering at 1 kV and annealing at ∼900 K. From the cleaned copper substrates, water desorption was also studied by the same procedures. All TPD spectra were obtained using a temperature ramp of ∼1.0 K/s.

Contact Angle Measurements. To prevent copper oxidation upon exposure to air, bare copper crystals were annealed at 500 °C in a hydrogen atmosphere. The contact angles were measured right after (i.e., within 1−2 min) and 30 min after annealing. When graphene is grown on a copper substrate (which was pre-annealed), it protects the copper surface from oxidation, and, therefore, no copper oxide layer was formed in the samples of graphene grown on copper. However, to remove the adsorbed airborne hydrocarbons,[17] all graphene samples were also annealed right before the contact angle measurements. Additional Raman spectra of the Cu samples were obtained after the removal of graphene by sputtering in UHV and re-exposing the samples to air.

AUTHOR INFORMATION

Corresponding Author

Grégory F. Schneider − *Faculty of Science, Leiden Institute of Chemistry, Leiden University, 2333CC Leiden, The*

https://doi.org/10.1021/acs.langmuir.0c02817
Langmuir 2021, 37, 4049−4055

Netherlands; orcid.org/0000-0002-3156-4525;
Email: g.f.schneider@chem.leidenuniv.nl

Authors

Liubov A. Belyaeva − *Faculty of Science, Leiden Institute of Chemistry, Leiden University, 2333CC Leiden, The Netherlands;* orcid.org/0000-0001-8958-9891

Chen Tang − *Faculty of Science, Leiden Institute of Chemistry, Leiden University, 2333CC Leiden, The Netherlands;* orcid.org/0000-0002-9512-2953

Ludo Juurlink − *Faculty of Science, Leiden Institute of Chemistry, Leiden University, 2333CC Leiden, The Netherlands;* orcid.org/0000-0002-5373-9859

Complete contact information is available at: https://pubs.acs.org/10.1021/acs.langmuir.0c02817

Notes

The authors declare no competing financial interest.

REFERENCES

(1) Shih, C.-J.; Strano, M. S.; Blankschtein, D. Wetting Translucency of Graphene. *Nat. Mater.* **2013**, *12*, 866−869.
(2) Parobek, D.; Liu, H. Wettability of Graphene. *2D Mater.* **2015**, *2*, 032001.
(3) Belyaeva, L. A.; Schneider, G. F. Wettability of Graphene. *Surf. Sci. Rep.* **2020**, *75*, 100482.
(4) Novoselov, K. S.; Morozov, S. V.; Jiang, D.; Zhang, Y.; Dubonos, S. V.; Grigorieva, I. V.; Firsov, A. A.; Electric Field, A. K. G. Electric Field Effect in Atomically Thin Carbon Films. *Science* **2004**, *306*, 666−669.
(5) Xu, Y.; Guo, Z.; Chen, H.; Yuan, Y.; Lou, J.; Lin, X.; Gao, H.; Chen, H.; Yu, B. In-Plane and Tunneling Pressure Sensors Based on Graphene/Hexagonal Boron Nitride Heterostructures. *Appl. Phys. Lett.* **2011**, *99*, 133109.
(6) Schedin, F.; Geim, A. K.; Morozov, S. V.; Hill, E. W.; Blake, P.; Katsnelson, M. I.; Novoselov, K. S. Detection of Individual Gas Molecules Adsorbed on Graphene. *Nat. Mater.* **2007**, *6*, 652−655.
(7) Heerema, S. J.; Dekker, C. Graphene Nanodevices for DNA Sequencing. *Nat. Nanotechnol.* **2016**, *11*, 127−136.
(8) Wang, Z.; Liu, C.-J. Preparation and Application of Iron Oxide/Graphene Based Composites for Electrochemical Energy Storage and Energy Conversion Devices: Current Status and Perspective. *Nano Energy* **2015**, *11*, 277−293.
(9) Yoon, J.-C.; Yoon, C.-S.; Lee, J.-S.; Jang, J.-H. Lotus Leaf-Inspired CVD Grown Graphene for a Water Repellant Flexible Transparent Electrode. *Chem. Commun.* **2013**, *49*, 10626−10628.
(10) Belyaeva, L. A.; van Deursen, P. M. G.; Barbetsea, K. I.; Schneider, G. F. Hydrophilicity of Graphene in Water through Transparency to Polar and Dispersive Interactions. *Adv. Mater.* **2018**, *30*, 1703274.
(11) Rafiee, J.; Mi, X.; Gullapalli, H.; Thomas, A. V.; Yavari, F.; Shi, Y.; Ajayan, P. M.; Koratkar, N. A. Wetting Transparency of Graphene. *Nat. Mater.* **2012**, *11*, 217−222.
(12) Taherian, F.; Marcon, V.; Van Der Vegt, N. F. A.; Leroy, F. What Is the Contact Angle of Water on Graphene? *Langmuir* **2013**, *29*, 1457−1465.
(13) Wang, S.; Zhang, Y.; Abidi, N.; Cabrales, L. Wettability and Surface Free Energy of Graphene Films. *Langmuir* **2009**, *25*, 11078−11081.
(14) Driskill, J.; Vanzo, D.; Bratko, D.; Luzar, A. Wetting Transparency of Graphene in Water. *J. Chem. Phys.* **2014**, *141*, 18C517.
(15) Shih, C.-J.; Wang, Q. H.; Lin, S.; Park, K.-C.; Jin, Z.; Strano, M. S.; Blankschtein, D. Breakdown in the Wetting Transparency of Graphene. *Phys. Rev. Lett.* **2012**, *109*, 176101.
(16) Ghaderi, N.; Peressi, M. First-Principle Study of Hydroxyl Functional Groups on Pristine, Defected Graphene, and Graphene Epoxide. *J. Phys. Chem. C* **2010**, *114*, 21625−21630.
(17) Li, Z.; Wang, Y.; Kozbial, A.; Shenoy, G.; Zhou, F.; McGinley, R.; Ireland, P.; Morganstein, B.; Kunkel, A.; Surwade, S. P.; Li, L.; Liu, H. Effect of Airborne Contaminants on the Wettability of Supported Graphene and Graphite. *Nat. Mater.* **2013**, *12*, 925−931.
(18) Yiapanis, G.; Makarucha, A. J.; Baldauf, J. S.; Downton, M. T. Simulations of Graphitic Nanoparticles at Air-Water Interfaces. *Nanoscale* **2016**, *8*, 19620−19628.
(19) Andrews, J. E.; Sinha, S.; Chung, P. W.; Das, S. Wetting Dynamics of a Water Nanodrop on Graphene. *Phys. Chem. Chem. Phys.* **2016**, *18*, 23482−23493.
(20) Prydatko, A. V.; Belyaeva, L. A.; Jiang, L.; Lima, L. M. C.; Schneider, G. F. Contact Angle Measurement of Free-Standing Square-Millimeter Single-Layer Graphene. *Nat. Commun.* **2018**, *9*, 4185.
(21) Raj, R.; Maroo, S. C.; Wang, E. N. Wettability of Graphene. *Nano Lett.* **2013**, *13*, 1509−1515.
(22) Smith, R. S.; Matthiesen, J.; Kay, B. D. Desorption Kinetics of Methanol, Ethanol, and Water from Graphene. *J. Phys. Chem. A* **2014**, *118*, 8242−8250.
(23) Chakradhar, A.; Burghaus, U. Adsorption of Water on Graphene/Ru(0001)—an Experimental Ultra-High Vacuum Study. *Chem. Commun.* **2014**, *50*, 7698−7701.
(24) Chakradhar, A.; Sivapragasam, N.; Nayakasinghe, M. T.; Burghaus, U. Support Effects in the Adsorption of Water on CVD Graphene: An Ultra-High Vacuum Adsorption Study. *Chem. Commun.* **2015**, *51*, 11463−11466.
(25) Ceyer, S. T. New Mechanisms for Chemistry at Surfaces. *Science* **1990**, *249*, 133−139.
(26) Chakradhar, A.; Trettel, K.; Burghaus, U. Benzene Adsorption on Ru(0001) and Graphene/Ru(0001)—How to Synthesize Epitaxial Graphene without STM or LEED? *Chem. Phys. Lett.* **2013**, *590*, 146−152.
(27) Chakradhar, A.; Sivapragasam, N.; Nayakasinghe, M. T.; Burghaus, U. Adsorption Kinetics of Benzene on Graphene: An Ultrahigh Vacuum Study. *J. Vac. Sci. Technol., A* **2016**, *34*, 021402.
(28) Wehling, T. O.; Lichtenstein, A. I.; Katsnelson, M. I. First-Principles Studies of Water Adsorption on Graphene: The Role of the Substrate. *Appl. Phys. Lett.* **2008**, *93*, 202110.
(29) King, D. A. Thermal Desorption from Metal Surfaces: A Review. *Surf. Sci.* **1975**, *47*, 384−402.
(30) Daschbach, J. L.; Peden, B. M.; Smith, R. S.; Kay, B. D. Adsorption, Desorption, and Clustering of H_2O on Pt(111). *J. Chem. Phys.* **2004**, *120*, 1516−1523.
(31) Stevenson, K. P.; Kimmel, G. A.; Dohnálek, Z.; Smith, R. S.; Kay, B. D. Controlling the Morphology of Amorphous Solid Water. *Science* **1999**, *283*, 1505−1507.
(32) Smith, R. S.; Petrik, N. G.; Kimmel, G. A.; Kay, B. D. Thermal and Nonthermal Physiochemical Processes in Nanoscale Films of Amorphous Solid Water. *Acc. Chem. Res.* **2012**, *45*, 33−42.
(33) Smith, R. S.; Matthiesen, J.; Knox, J.; Kay, B. D. Crystallization Kinetics and Excess Free Energy of H_2O and D_2O Nanoscale Films of Amorphous Solid Water. *J. Phys. Chem. A* **2011**, *115*, 5908−5917.
(34) Orlova, E.; Feoktistov, D.; Kuznetsov, G. Investigation of Drop Dynamic Contact Angle on Copper Surface. *EPJ Web Conf.* **2015**, *82*, 01053.
(35) Yekta-fard, M.; Ponter, A. B. Surface Treatment and Its Influence on Contact Angles of Water Drops Residing on Teflon and Copper. *J. Adhes.* **1985**, *18*, 197−205.
(36) Li, R.; Huang, Z.; Wu, X.; Yan, P.; Dai, X. Cryogenic Quenching of Rock Using Liquid Nitrogen as a Coolant: Investigation of Surface Effects. *Int. J. Heat Mass Transfer* **2018**, *119*, 446−459.
(37) Schrader, M. E. Ultrahigh Vacuum Techniques in the Measurement of Contact Angles. III. Water on Copper and Silver. *J. Phys. Chem.* **1974**, *78*, 87−89.
(38) Gottardi, S.; Müller, K.; Bignardi, L.; Moreno-López, J. C.; Pham, T. A.; Ivashenko, O.; Yablonskikh, M.; Barinov, A.; Björk, J.;

Rudolf, P.; Stöhr, M. Comparing Graphene Growth on Cu(111) versus Oxidized Cu(111). *Nano Lett.* **2015**, *15*, 917−922.
(39) Luo, D.; You, X.; Li, B.-W.; Chen, X.; Park, H. J.; Jung, M.; Ko, T. Y.; Wong, K.; Yousaf, M.; Chen, X.; Huang, M.; Lee, S. H.; Lee, Z.; Shin, H.-J.; Ryu, S.; Kwak, S. K.; Park, N.; Bacsa, R. R.; Bacsa, W.; Ruoff, R. S. Role of Graphene in Water-Assisted Oxidation of Copper in Relation to Dry Transfer of Graphene. *Chem. Mater.* **2017**, *29*, 4546−4556.
(40) Lu, J.-Y.; Olukan, T.; Tamalampudi, S. R.; Al-Hagri, A.; Lai, C.-Y.; Ali Al Mahri, M.; Apostoleris, H.; Almansouri, I.; Chiesa, M. Insights into Graphene Wettability Transparency by Locally Probing Its Surface Free Energy. *Nanoscale* **2019**, *11*, 7944−7951.
(41) Doering, D. L.; Madey, T. E. The Adsorption of Water on Clean and Oxygen-Dosed Ru(011). *Surf. Sci.* **1982**, *123*, 305−337.
(42) Colbourn, E.; Hadden, R. A.; Vandervell, H. D.; Waugh, K. C.; Webb, G. Adsorption of Water on Polycrystalline Copper: Relevance to the Water Gas Shift Reaction. *J. Catal.* **1991**, *130*, 514−527.
(43) Trotochaud, L.; Head, A. R.; Pletincx, S.; Karslıoğlu, O.; Yu, Y.; Waldner, A.; Kyhl, L.; Hauffman, T.; Terryn, H.; Eichhorn, B.; Bluhm, H. Water Adsorption and Dissociation on Polycrystalline Copper Oxides: Effects of Environmental Contamination and Experimental Protocol. *J. Phys. Chem. B* **2018**, *122*, 1000−1008.
(44) Liu, Q.; Li, J.; Tong, X.; Zhou, G. Enhancing Dissociative Adsorption of Water on Cu(111) via Chemisorbed Oxygen. *J. Phys. Chem. C* **2017**, *121*, 12117−12126.
(45) Yamamoto, S.; Andersson, K.; Bluhm, H.; Ketteler, G.; Starr, D. E.; Schiros, T.; Ogasawara, H.; Pettersson, L. G. M.; Salmeron, M.; Nilsson, A. Hydroxyl-Induced Wetting of Metals by Water at Near-Ambient Conditions. *J. Phys. Chem. C* **2007**, *111*, 7848−7850.
(46) Arjmandi-Tash, H.; Belyaeva, L. A.; Schneider, G. F. Single Molecule Detection with Graphene and Other Two-Dimensional Materials: Nanopores and Beyond. *Chem. Soc. Rev.* **2016**, *45*, 476−493.
(47) Li, X.; Cai, W.; An, J.; Kim, S.; Nah, J.; Yang, D.; Piner, R.; Velamakanni, A.; Jung, I.; Tutuc, E.; Banerjee, S. K.; Colombo, L.; Ruoff, R. S. Large-Area Synthesis of High-Quality and Uniform Graphene Films on Copper Foils. *Science* **2009**, *324*, 1312−1314.
(48) Suk, J. W.; Kitt, A.; Magnuson, C. W.; Hao, Y.; Ahmed, S.; An, J.; Swan, A. K.; Goldberg, B. B.; Ruoff, R. S. Transfer of CVD-Grown Monolayer Graphene onto Arbitrary Substrates. *ACS Nano* **2011**, *5*, 6916−6924.
(49) Badan, C.; Koper, M. T. M.; Juurlink, L. B. F. How Well Does Pt(211) Represent Pt[n(111) × (100)] Surfaces in Adsorption/Desorption? *J. Phys. Chem. C* **2015**, *119*, 13551−13560.
(50) den Dunnen, A.; van der Niet, M. J. T. C.; Koper, M. T. M.; Juurlink, L. B. F. Interaction between H_2O and Preadsorbed D on the Stepped Pt(553) Surface. *J. Phys. Chem. C* **2012**, *116*, 18706−18712.

NOTE ADDED AFTER ASAP PUBLICATION

This article published ASAP on March 2, 2021. Text changes have been made and the corrected version reposted on March 29, 2021.

https://doi.org/10.1021/acs.langmuir.0c02817
Langmuir 2021, 37, 4049−4055